Spatial aliasing removal using deep learning super-resolution

Garg, A.; Vos, A.; Bortych, N.; Gupta, D. K.; Verschuur, D. J.

DOI
10.3997/1365-2397.n0057

Publication date
2019

Document Version
Final published version

Published in
First Break

Spatial aliasing removal using deep learning super-resolution

A. Garg[1]*, A. Vos[2], N. Bortych[2], D.K. Gupta[2] and D.J. Verschuur[1] use a deep learning super-resolution network to upscale the data by a factor of two in the spatial direction and remove the spatial aliasing present in the data.

Introduction

Seismic data are often either irregularly or insufficiently sampled. Irregular sampling can be due to encountered obstacles in the acquisition, thus resulting in a seismic data gap, whereas insufficient sampling is the result of a coarse acquisition grid, thus leading to sparse sampling along the spatial direction of the data. This irregular or insufficient sampling can affect the accuracy and resolution of seismic data processing steps such as surface-related multiple elimination, migration and inversion. For example, in the simple case of sparse sampling, it leads not just to the loss of high-wavenumbers, but also causes spatial aliasing due to the overlap of aliasing energy artifacts with the signal energy. When we image this spatially aliased coarse data, we encounter the trade-off between the resolution of the image and the aliasing artifacts. Therefore, seismic data interpolation has always been an essential requirement in seismic data processing.

There are different kinds of interpolation methods, such as transform-based methods (Spitz, 1991; Gulunay, 2003; Liu and Sacchi, 2004), rank-reduction-based methods (Trickett et al., 2010) and wave-equation-based methods (Fomel, 2003), used to account for spatial sampling issues. However, most of these methods are more suitable for the irregularly sampled or randomly missing data case. For regularly sampled seismic data with the spatial aliasing effects, an anti-aliasing interpolation strategy has to be adopted in these methods to improve the interpolation performance. These methods' accuracy is not just sensitive to the choice of the selected parameters, but in methods where they characterize the data in the linear way, they are also affected by the complexity in the seismic data.

Deep learning (LeCun et al., 2015) has gained a lot of attention in recent years because of its ability to extract deeper low-level features from the data in a non-linear setting by self-learning. Deep learning approaches like convolutional neural networks (CNN) (Krizhevsky et al., 2012) have proven particularly adept at image processing tasks such as de-noising and super-resolution (Yang et al., 2019). Super-resolution refers to the task of upscaling and improving the details in images, which leads to the image resolution enhancement. Even in the seismic community, several attempts have been made to mitigate the problem of limited resolution data using CNNs. For example, Halpert (2018) uses CNN-based generative adversarial network (GAN) (Goodfellow et al., 2014) to produce high-resolution realizations of low-resolution input seismic images.

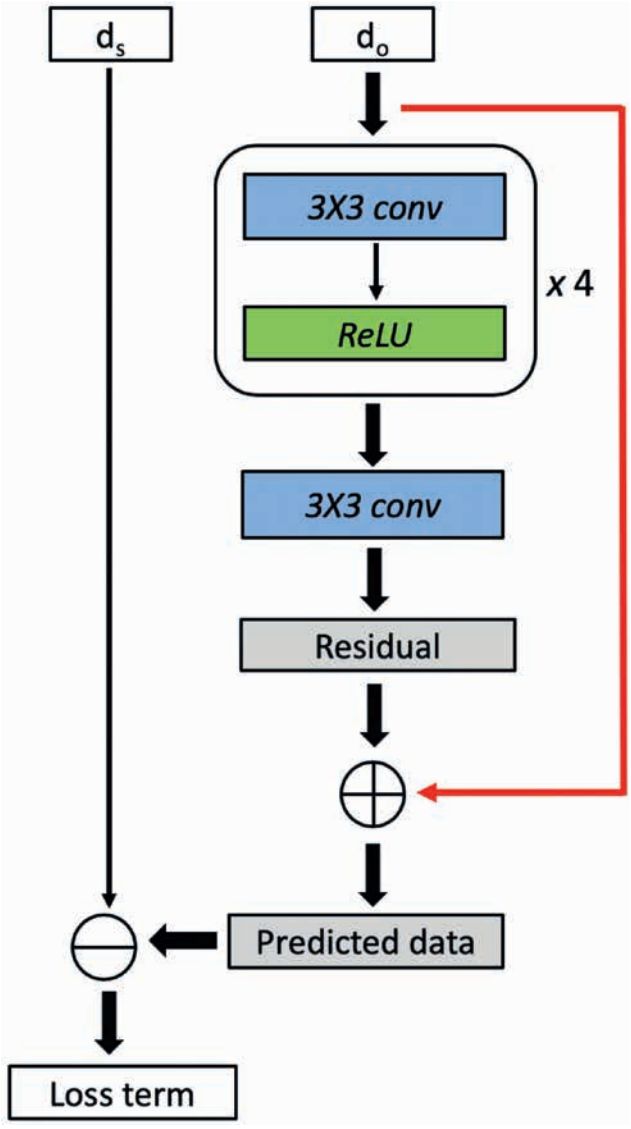

Figure 1 Modified very deep super-resolution (VDSR) network architecture (Kim et al., 2016).

[1] Delft University of Technology | [2] University of Amsterdam
* Corresponding author, E-mail: aayushgargiitr@gmail.com

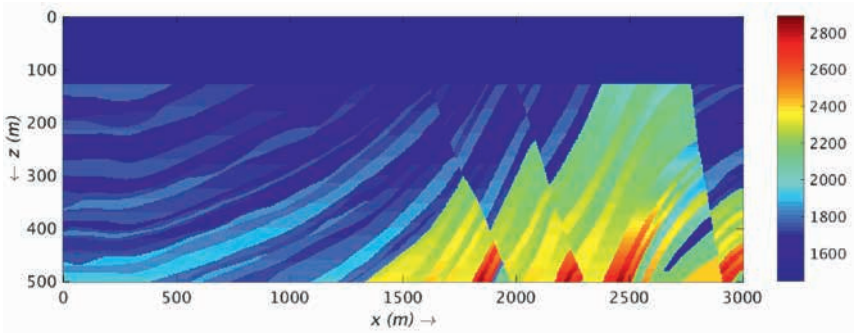

Figure 2 Subsurface velocity model used to generate the data for training the network.

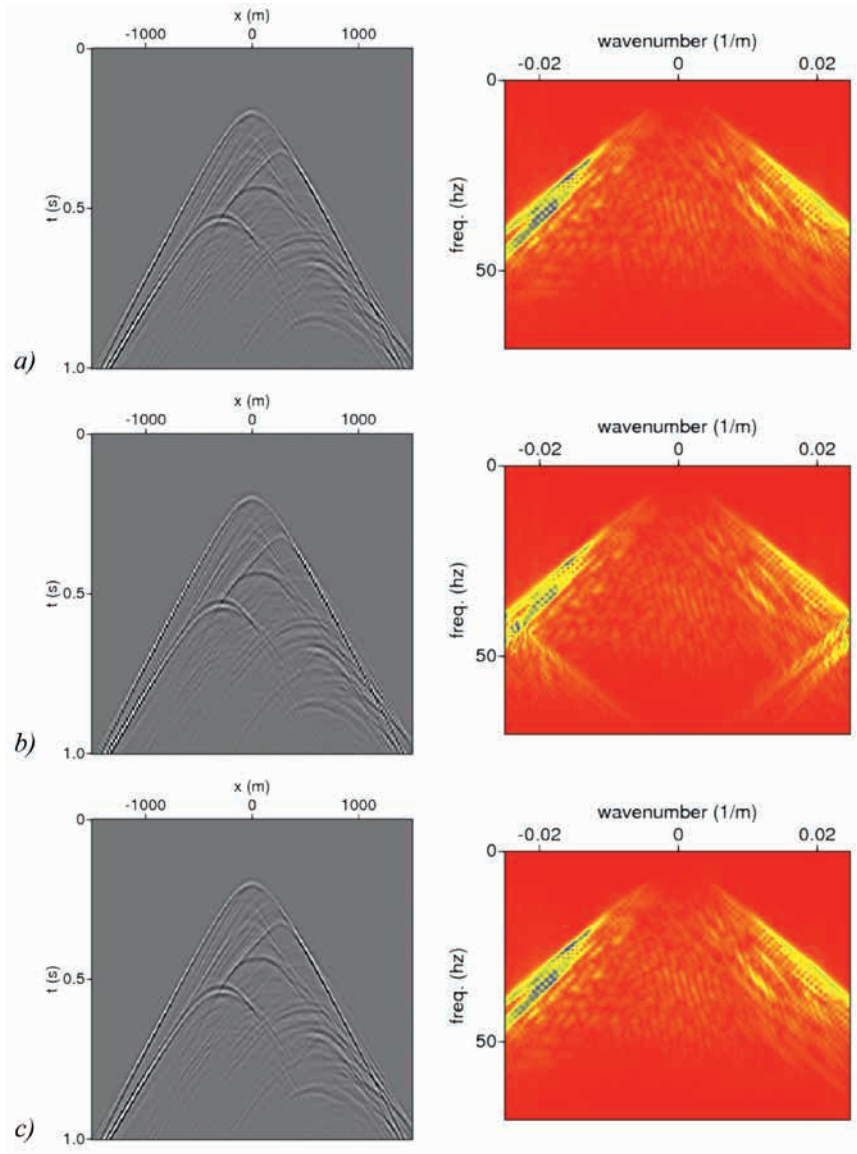

Figure 3 The shot data in x-t (left) and f-k domain (right) from the test dataset. a) High-resolution unaliased dense output data, b) low-resolution aliased input data and c) reconstructed dense data with aliasing removed using the trained network.

In this article, we use deep learning super-resolution to apply seismic data anti-aliasing interpolation and reconstruct accurate dense seismic data. We make use of a modified version of the so-called very deep super-resolution (VDSR) network (Kim et al., 2016) to upscale the data by a factor of two in the spatial direction and remove the spatial aliasing present in the data. Moreover, in order to make the network robust, we use a loss function that minimizes the error both in the space-time (*x-t*) and in the frequency-wavenumber (*f-k*) domain as spatial aliasing is much more visible in the *f-k* domain. We train the network using the data generated for a part of the Marmousi model and use the data from the Sigsbee model as a blind test to demonstrate its ability to generalize. Also, for quality check, we apply imaging to both the input (spatially aliased) and the upscaled output (free of spatial aliasing) data for both training and blind cases to show the improvement in the seismic image. We show that the trained network is able to reconstruct the dense data with half the receiver interval and remove the spatial aliasing in the *f-k* domain.

Note, we make all the codes and datasets used to train the network and generate the results for this article freely available. It can be downloaded from https://github.com/garg-aayush/spatial-alias-removal/.

Method

The first attempt at the super-resolution problem using deep learning was the super-resolution CNN (SRCNN) network (Dong et al., 2015). Even though the model was relatively shallow, it developed the interest in the problem of single image super-resolution in the field of deep learning. Thereafter, Kim et al (2016) used a VGG-style 20-layer network for the super-resolution problem and exploited the depth of the network to achieve better performance. Importantly, they used a residual approach, i.e., adding the image to the output of the network, so the network learns only the residual function instead of the full transformation. This residual learning helps to avoid the vanishing gradient problem in deeper layers and is useful for training the network with a high reconstruction accuracy. We make use of a modified, smaller version of the VDSR network for our spatial aliasing removal problem.

Network architecture

Figure 1 shows the used modified version of the VDSR network. The network contains four blocks, each with a convolution layer of 128 filters with 3x3 size followed by rectified linear activation function (*ReLU*), and a convolution layer of 128 filters with 3x3 size. In Figure 1, the term d_o denotes the low-resolution aliased input data whereas d_s represents the super-resolution unaliased output data during the training. To ensure that the low-resolution input data has the same dimensionality as the super-resolution data, the d_o is initially interpolated using bilinear interpolation. Also, in Figure 1, we see that our modified VDSR network's property of trying to learn the residual function ($d_o - d_s$) rather than ($d_o \rightarrow d_s$) mapping.

	GAN discriminator loss			
	✓	✗		
L2 loss	13	52.1	✓	f-k
	29.5	52.2	✗	
L1 loss	13	56.0	✓	f-k
	43.7	51.0	✗	

Table 1 PSNR (in dBs) based on the grid search over the reconstruction loss and the loss spaces.

Loss function

We make use of a L1 loss function that minimizes the error both in space-time (*x-t*) and frequency-wavenumber (*f-k*) domain as spatial aliasing is much more visible in the *f-k* domain. This way, during the optimization, the network is forced to reduce the visual spatial aliasing artifacts in both the domains. It eventually makes the network more robust and helps to attain better signal-to-noise (S/N) ratio. The used loss function can be written as:

$$L(\Theta) = \tfrac{1}{2} \| f(d_o;\Theta) - d_s \|_1 + \tfrac{1}{2} \| f(d_o;\Theta)_{f-k} - d_{s,f-k} \|_1, \qquad (1)$$

where f represents the used network, subscript *f-k* represents the *f-k* transforms and Θ represents the network model parameters. Note that we avoided using the popular generative adversarial

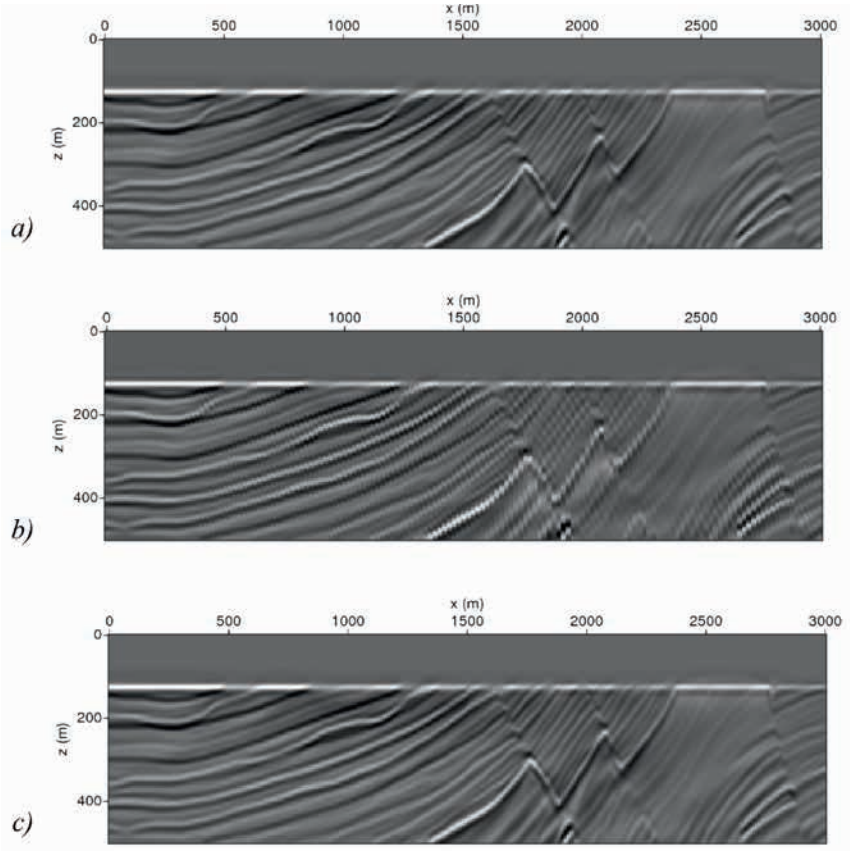

Figure 4 Migrated seismic images obtained for the marmousi dataset. Image for the a) high-resolution unaliased dense output data, b) low-resolution aliased input data and c) reconstructed dense data with aliasing removed using the trained network.

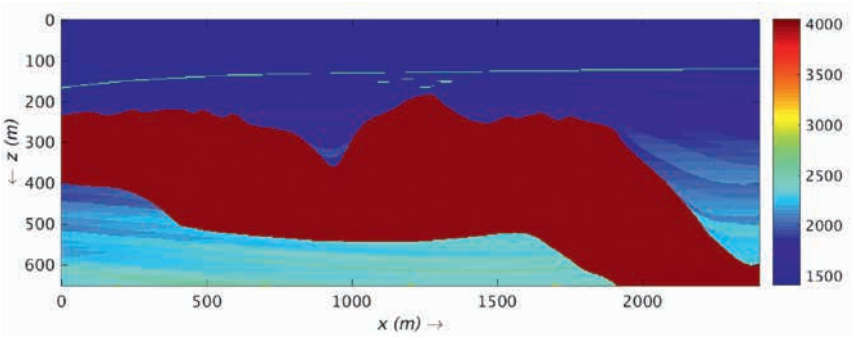

Figure 5 Subsurface velocity model used to generate the blind dataset.

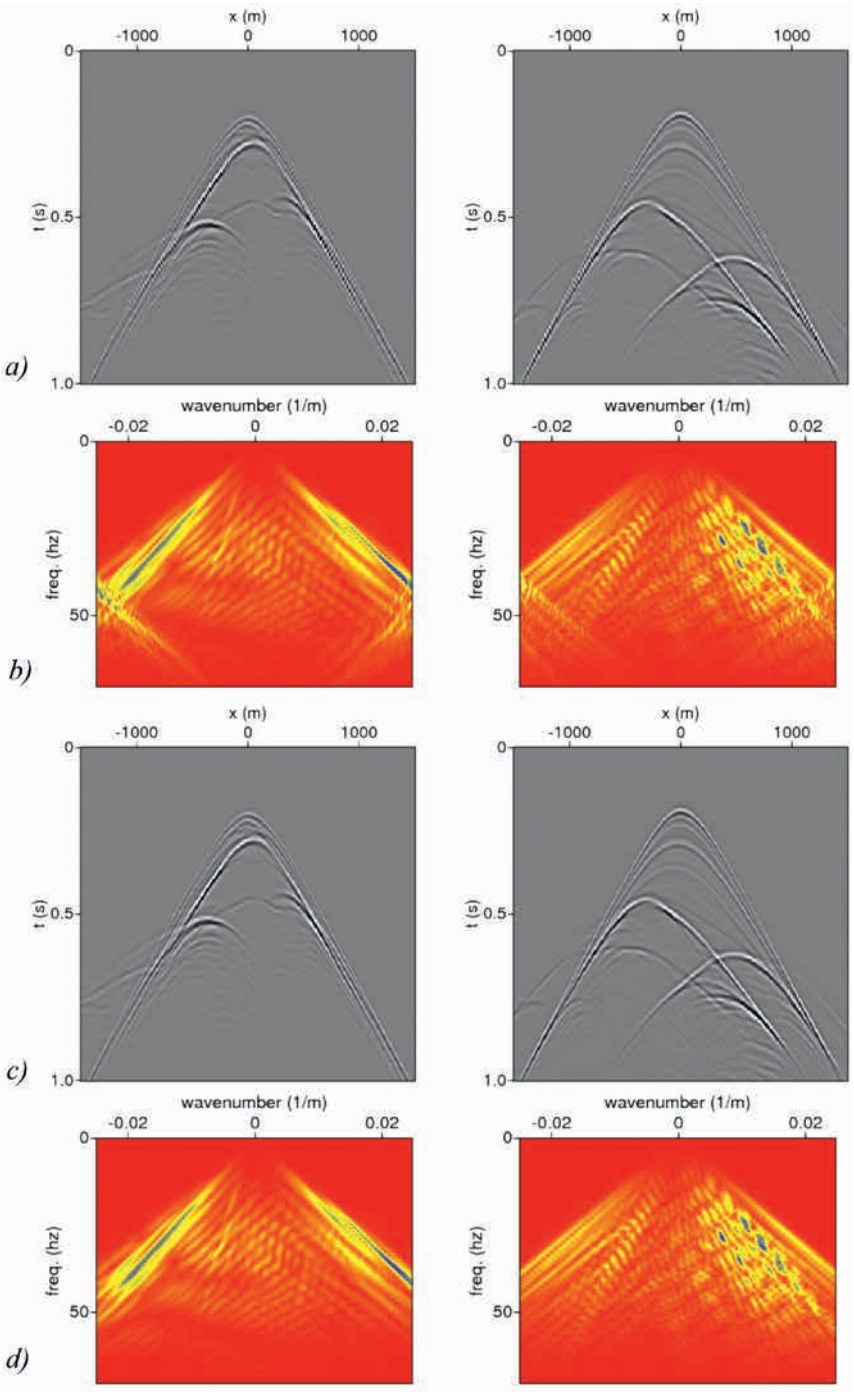

Figure 6 The two shots in the a), c) x-t and the b), d) f-k domain. The a), b) low-resolution aliased input blind data and the corresponding b), d) reconstructed dense data with aliasing removed using the trained network.

networks (GAN) discriminator loss (Goodfellow et al., 2014) due to its adversarial nature. At times, it is also notoriously difficult to train, thus requiring a number of heuristics to solve (Arjovsky and Bottou, 2017).

Evaluation metrics

Since the problem is modelled as single image super-resolution, we use two metrics that are widely used in the super-resolution field (Yang et al., 2019): peak signal-to-noise ratio (*PSNR*) and structural similarity index method (*SSIM*). Given two images with the same dimensions, I_1 and I_2, the *PSNR* is computed in following way:

$$MSE = \frac{1}{N} \| I_1 - I_2 \|_F^2 , \quad (2)$$

$$PSNR\ (in\ dB) = 10 log_{10} \left(\frac{L^2}{MSE} \right) , \quad (3)$$

where N is the number of pixels, F being the Frobenius norm and L being the maximum value of the pixel, which is 1 in our case. The SSIM is defined as follows:

$$SSIM\ (I_1, I_2) = \frac{2\mu_{I_1}\mu_{I_2} + k_1}{\mu_{I_1}^2 + \mu_{I_2}^2 + k_1} \cdot \frac{\sigma_{I_1}\sigma_{I_2} + k_2}{\sigma_{I_1}^2 + \sigma_{I_2}^2 + k_2} , \quad (4)$$

where μ and σ are the mean and variance of corresponding image, $\sigma_{I_1 I_2}$ is covariance between the two images and k's are constants. Note, for our case I_1 and I_2 are unaliased ideal output data and network reconstructed dense data, respectively.

Training the network

We generate 400 shot records for receiver sampling of 20 m and 10 m using the finite-difference method for part of the Marmousi model shown in Figure 2. The shot record of size 256 X 151 with 20 m receiver sampling acts as the input low-resolution spatially aliased data whereas the corresponding 10 m receiver sampling data of size 256 X 301 acts as the output high-resolution spatially unaliased data for training the network. Note that we split the total dataset randomly into test, validation and train set of 10%, 10% and 80% each during the training. Figures 3a and 3b show the output and the input data, respectively, from the test set in both *x-t* and *f-k* domain.

The training was carried out on the Pytorch platform (Paszke et al., 2017). We experimented with different combinations of hyperparameters such as number of epochs, learning rate, type of reconstruction loss, number of filters, filter size, batch size, etc. Eventually, we tuned the network shown in Figure 1 to have a PSNR of 59 dB and *SSIM* of 0.999 on the validation set. More details on hyperparameter tuning and the final choice of hyperparameters can be found in the shared github repository.

After we tuned the network, the test set was used to assess the network performance. The trained network was able to achieve the *PSNR* of 56 dB and *SSIM* of 0.999 for the test dataset in comparison to the baseline (d_o) *PSNR* of 26 dB and *SSIM* of 0.92. Figure 3c shows a reconstructed test dataset shot and its *f-k* transform using the trained network. The reconstructed super-resolution shot record (Figure 3c) with half the receiver sampling has much more continuity in time and space and is identical to the unaliased output labelled data. Similarly, we also see the spatial aliasing disappearing in the *f-k* domain of the reconstructed test dataset shot record.

We also performed a grid search over the reconstruction loss terms, while keeping the other hyperparameters constant, to get an understanding of the influence of these hyperparameters. From the results shown in Table 1, we clearly show the maximum *PSNR* is achieved for the L1 loss terms (using both *x-t* and *f-k* domain) without using the GAN discriminators loss for the current used network.

As a final quality check, to see the effects of aliasing in the seismic imaging, we apply the pre-stack depth migration to all the three datasets (aliased input data, unaliased output data, reconstructed data) and obtain the subsurface migrated image for each of them (Figure 4). In Figure 4b, we clearly see the effect of coarse sampling and spatial aliasing in terms of unimaged steep dips and aliasing artifacts. On the other hand, the migrated image obtained for the upscaled reconstructed data (Figure 4c) is of much higher resolution and consistent with what we would have obtained by using unaliased output data (Figure 4a).

Blind dataset results

To assess the performance and generality of any trained network, the blind test using data with different features is of the utmost importance. We generate 200 shots for receiver sampling of 20 m using a part of the Sigsbee model shown in Figure 5 and use the trained network to get the reconstructed data upscaled by a factor of two in the spatial direction. Figure 6 shows the shot records for input low-resolution spatially aliased blind data

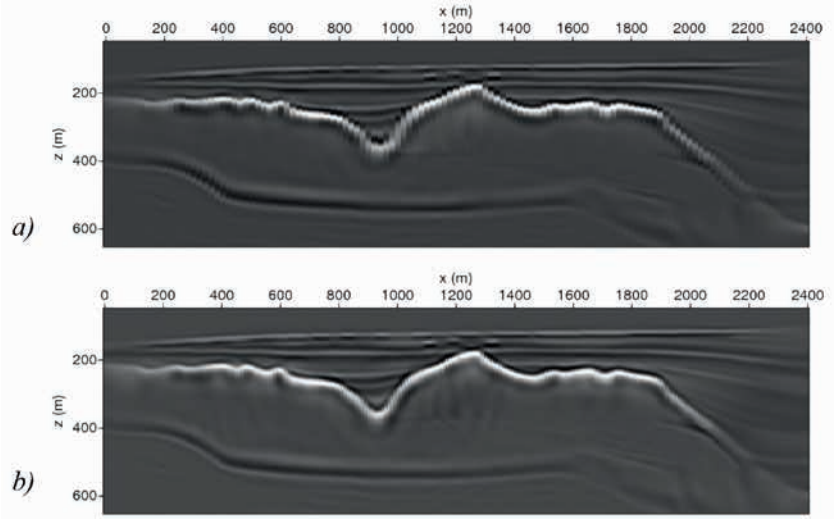

Figure 7 Migrated seismic images obtained for the a) low-resolution aliased input blind dataset and the corresponding b) reconstructed dense data with aliasing removed using the trained network.

and the reconstructed super-resolution data in both *x-t* and *f-k* domain. Even for the blind dataset, we see the spatial aliasing disappears in the *f-k* domain of the reconstructed data and it has much more continuity and a lot less visual pixelation along the spatial axis. The similar effects can be seen in the migrated images (see Figure 7) obtained using both the datasets. The obtained migrated image via reconstructed dense super-resolution data (Figure 7b) has much more continuity and clearly imaged steep events in comparison to one obtained via coarse aliased input data (Figure 7a). This blind test further demonstrates the accuracy and the validity of the trained network.

Discussion

Though we have shown the promising blind test results, we can still expect the network performance to suffer for data with higher complexity features. For example, in this study, we restricted ourselves to noise-free data, thus we can expect the results to suffer for noisy test data. However, the network can be made more general by training a larger network with different datasets. Also, we only showed the case of upscaling by a factor of two, upscaling by larger factors and more severe spatial aliasing still needs to be assessed. In any case, the proposed network can be used as the initial network for the transfer learning (Shin et al., 2016) process in order to obtain a more general network for spatial aliasing removal.

Conclusions

We used a deep learning super-resolution network to upscale the input data by a factor of two and remove the spatial aliasing present in the data. We trained a modified VDSR network and assessed its performance both qualitatively and quantitatively. We showed that using a loss function that minimizes error not just in *x-t* domain but also in *f-k* domain helps to get a robust network with higher *PSNR*, as shown in the grid search for reconstruction loss and loss type experiment. The reconstructed data with half the receiver interval in both the training and the blind test case showed more continuity and less visual pixilation with the spatial aliasing removed in the *f-k* domain. The effects of reconstructed dense data were also in seismic imaging with the obtained migrated image having more continuity and clearly imaged steep events in comparison to one obtained via coarse aliased input data.

The presented type of deep learning network for anti-aliasing interpolation, with more extensive research, has the potential to develop into an effective strategy for the spatial aliasing removal and dense data reconstruction for large volumes of coarse data.

Acknowledgements

A. Garg and D.J. Verschuur thank the members of the Delphi Consortium for their support. The authors would also like to thank the French Institute of petroleum (IFP) and SMAART JV for the Marmousi and the Sigsbee model, respectively.

Data and code availability

All the data and codes used to develop the results for this article can be downloaded from https://github.com/garg-aayush/spatial-alias-removal

References

Arjovsky, M., Chintala, S. and Bottou, L. [2017]. Wasserstein Generative Adversarial Networks. *34th International Conference on Machine Learning*, PMLR 70,214-223.

Dong, C., Loy, C.C., He, K. and Tang, X. [2015]. Image super-resolution using deep convolutional networks. *IEEE transactions on pattern analysis and machine intelligence*, **38**(2), 295-307.

Fomel, S. [2003]. Seismic reflection data interpolation with differential offset and shot continuation. *Geophysics*, **68**, 733-744.

Goodfellow, I., Pouget-Abadie, J., Mirza, M., Xu, B., Warde-Farley, D., Ozair, S. and Bengio, Y. [2014]. Generative adversarial nets. *Advances in neural information processing systems*, 2672-2680.

Gulunay, N. [2003]. Seismic trace interpolation in the Fourier transform domain. *Geophysics*, **68**, 355-369.

Halpert, A.D. [2018]. Deep learning-enabled seismic image enhancement. *88th SEG Annual International Meeting*, Expanded Abstracts, 2081-2085.

Kim, J.J., Lee, K. and Lee, K. M. [2016]. Accurate image super-resolution using very deep convolutional networks. *IEEE Conference on Computer Vision and Pattern Recognition*, 1646-1654.

Krizhevsky, A., Sutskever, I. and Hinton, G.E. [2012]. ImageNet classification with deep convolutional neural networks. *25th International Conference on Advances in Neural Information Processing Systems*, 1097-1105.

LeCun, Y., Bengio, Y. and Hinton, G. [2015]. Deep learning. *Nature*, **521**, 436-444.

Liu, B. and Sacchi, M. [2004]. Minimum weighted norm interpolation of seismic records. *Geophysics*, **69**, 1560-1568.

Paszke, A., Gross, S., Chintala, S., Chanan, G., Yang, E., DeVito, Z., Lin, Z., Desmaison, A., Antiga, L. and Lerer, A. [2017]. *Automatic differentiation in PyTorch.* NIPS Autodiff Workshop: The Future of Gradient-based Machine Learning Software and Techniques.

Shin, H.C., Roth, H.R., Gao, M., Lu, L., Xu, Z., Nogues, I., Yao, J., Mollura, D., Summers, R.M. [2016]. Deep convolutional neural networks for computer-aided detection. CNN architectures, dataset characteristics and transfer learning. *IEEE Transactions on Medical Imaging*, **35**(5), 1285-1298.

Spitz, S. [1991]. Seismic trace interpolation in the F-X domain. *Geophysics*, **56**, 785-794.

Trickett, S., Burroughs, L., Milton, A., Walton, L. and Dack R. [2010]. Rank reduction-based trace interpolation. *80th SEG Annual International Meeting*, Expanded Abstracts, 3829–3833.

Yang, W., Zhang, X., Tian, Y., Wang, W. and Xue, J. [2019]. Deep learning for single image super-resolution: A brief review. *IEEE Transactions on Multimedia,* under review.